Topographic effects on solar radiation distribution in mountainous watersheds and their influence on reference evapotranspiration estimates at watershed scale

C. Aguilar[1], J. Herrero[2] and M.J. Polo[1]

[1]{Fluvial Dynamics and Hydrology Research Group, University of Córdoba, Spain}

[2]{ Fluvial Dynamics and Hydrology Research Group, University of Granada, Spain }

Correspondence to: C. Aguilar (caguilar@uco.es)

Abstract

Distributed energy and water balance models require time-series surfaces of the climatological variables involved in hydrological processes. Among them, solar radiation plays an important role, especially in arid environments, as it is a key variable to the circulation of water in the atmosphere. The lack of reliable data for the assessment of solar radiation has led to the use of models. Most of the hydrological GIS-based models apply simple interpolation techniques to data measured at sparse meteorological stations disregarding topographic effects. Here, a topographic solar radiation algorithm is included for the generation of detailed time-series solar radiation surfaces using limited data and relatively simple methods, in order to quantify the effects of topography on the water losses through evapotranspiration estimates in a mountainous watershed in southern Spain. First, the comparison between the topographically corrected interpolated values of daily solar radiation and those obtained by a direct spatial interpolation technique (Inverse Distance Weighed, IDW) is provided. The results show the major role of topography in local values and differences of up to +60% and -90% in the estimated daily values. Besides, the results are compared to experimental data proving the usefulness of the model for the estimation of spatially distributed radiation values in complex terrain, with a good adjustment for daily values and the best fits under cloudless skies at hourly time steps. Finally, evapotranspiration fields estimated through the ASCE-Penman-Monteith equation using both corrected and non-corrected radiation values address the hydrologic importance of using topographically

corrected solar radiation fields as inputs to the equation over uniform values with mean differences in the watershed of 62 mm/year and 142 mm/year of standard deviation. High speed computations in a 1300 km^2 watershed in the south of Spain with up to a one-hour time scale in 30 x 30 m^2 cells can be easily carried out on a desktop PC.

1 Introduction

There are several methods available for the development of digital elevation models for hydrological studies but regular grid structures provide the best compromise between accuracy and computational efficiency (Moore et al., 1991). For this, all the inputs to distributed hydrological modelling must be available at this spatial scale. Among such inputs to hydrological models, solar radiation plays an important role in most of the processes involved, as it is a key variable in the circulation of water from the earth's surface to the atmosphere, especially at Mediterranean regions. At a global scale, latitudinal gradients caused by the earth's rotation and translation movements are well-known. However, at a smaller scale, apart from cloudiness and other atmospheric heterogeneities, topography determines the distribution of the incoming solar radiation; variability in slope angle and slope orientation, as well as the shadows cast by topographic agents, can lead to strong local gradients in solar radiation (Dozier, 1980; Dubayah, 1992; Dubayah and van Katwijk, 1992), with the corresponding influence on the energy-mass balance of the snow cover and its evolution (Dubayah and van Katwijk, 1992; Herrero et al., 2009), the vegetation canopy (Dubayah, 1994), the surface soil layer, surface water bodies, etc.

The regional climate in Mediterranean areas is characterized by great inland-coast, valley-hill contrasts, and is subject to cyclical fluctuations in cloud cover, precipitation and drought, thus exhibiting considerable spatial and temporal variations (Diodato and Bellocchi, 2007). In such latitudes, during periods of lack of rainfall - a common event at different spatial and temporal scales - radiation is the main force in the system which causes both snowmelt and evapotranspiration. Here, an accurate estimation of time-series solar radiation surfaces is required for distributed energy and water balance modelling (Ranzi and Rosso, 1995; Herrero et al., 2007).

One of the main drawbacks in the assessment of solar radiation is the lack of reliable data. In mountainous areas where the monitoring network ineffectively covers the complex heterogeneity of the terrain, simple geostatistical methods for spatial interpolation are not

always representative enough, and algorithms that explicitly or implicitly account for the features creating strong local gradients in the incoming radiation must be applied (Susong et al., 1999; Garen and Marks, 2005; Chen et al., 2007). Thus, the implementation of the spatial variability in the incoming radiation at the cell scale for distributed hydrological modelling is of major concern, especially in mountainous areas (Allen et al., 2006). Here, the combination of extreme gradients in the spatial distribution of solar radiation, together with the lack of measurements at detailed spatial and temporal scales, calls for the integration of algorithms simple enough to be run with common measurements but at the same time able to capture the agents that constitute the main sources of the spatial and temporal variability of solar radiation.

At the local scale, the amount of solar radiation reaching a given location is called global solar radiation and it depends mainly on the cloud cover, the turbidity of the clean air, the time of the year, latitude, and surface geometry (Iqbal, 1983; Essery and Marks, 2007). As radiation penetrates the atmosphere, it is depleted by absorption and scattering. Not all of the scattered radiation is lost, since part of it eventually arrives at the surface of the earth in the form of diffuse radiation (Liu and Jordan, 1960). Global radiation is the sum of direct or beam irradiance from the sun, diffuse irradiance from the sky, where a portion of the overlying hemisphere may be obstructed by the terrain, and direct and diffuse irradiance reflected by nearby terrain (Dubayah, 1994). Therefore, global radiation received on a surface with a random slope and aspect is largely controlled by atmospheric and topographic conditions (Flint and Childs, 1987; Tian et al., 2001; Diodato and Bellocchi, 2007). In very rough terrain, some areas may not receive any direct radiation during the whole year - even if facing south - because of high peaks surrounding them. Under such conditions, a GIS-based solar radiation model that considers the impact of terrain shading should be applied (Allen et al., 2006).

In any case, for the estimation of radiation incident on tilted surfaces, the partition of global horizontal radiation into its beam and diffuse components is of major concern, as the topographic effects are different for each one and therefore have to be modelled separately (Iqbal, 1980; Antonic, 1998; González-Dugo et al., 2003). Thus, diffuse radiation is affected by the unobstructed portion of the overlying hemisphere while reflected radiation is affected by terrain slope and the portion of the overlying hemisphere obstructed by terrain (Dubayah, 1994). As for the beam component, self-shadowing and shadows cast by surrounding terrain have to be considered for each sun position in the sky during the day.

For the quantification of the diffuse component, many parameters related to the atmospheric properties are required in order to express the scattering properties of the atmosphere. However, these parameters are not easily available or their computation from common measurements may be time-consuming (Dubayah and van Katwijk, 1992) and so simpler procedures need to be applied, especially at watershed scale and rough terrain. Thus, in these situations the basic procedure for the partition of global radiation into its components is the calculation of correlations between the daily global radiation and its diffuse component from measured values of both quantities, and then to apply such correlations at locations where diffuse radiation data are not available (Iqbal, 1980). In the literature there are several reviews about the different correlations available, depending on the averaging procedure and on the time scale of the radiation data (e.g. hourly or daily) (Iqbal, 1980; Spencer, 1982; Kambezidis et al., 1994; Jacovides et al., 1996). Liu and Jordan (1960) were the first authors to develop a model for the estimation of diffuse radiation from global data, establishing the basis for later empirical analysis of global radiation from daily data. Ruth and Chant (1976) obtained a very similar figure and demonstrated a latitudinal dependence in the models. Other authors developed hourly correlations (Orgill and Hollands, 1977; Bugler, 1977; Erbs et al., 1982). In 1979 Collares-Pereira and Rabl, maintaining the assumption of isotropic approximation for the diffuse radiation previously proposed by Liu and Jordan, improved some aspects of the model (correction for the shade ring effect and use of daily values for extraterrestrial radiation instead of single monthly values) and defined the daily clearness index as the ratio of global radiation to extraterrestrial radiation.

Despite the availability of topographically corrected models for the estimation of solar radiation fields as Dozier and Frew (1980), Dubayah (1992, 1994), etc., these approaches are not commonly included in GIS-based hydrological models. On the contrary, most GIS-based hydrological models usually adopt simple approaches to estimate the incident radiation throughout the watershed. In AnnAGNPS, a distributed-parameter, physically- based, continuous-simulation, watershed-scale, nonpoint-source pollutant model (Cronshey and Theurer, 1998), correction factors to take account of the effects of dust, water vapour, path length, and reflection and rescattering are applied to the extraterrestrial radiation in order to obtain the short wave radiation received at the ground surface. However these corrections are simplified into two multiplicative factors, one reflecting the effects of the atmosphere as a function of the elevation and another as the influence of clouds, which depends on the percentage of possible sunshine for each day (Bingner and Theurer, 2003). Land area

representations of a watershed are used to provide landscape spatial variability, so climatic variables remain constant at a subwatershed scale and therefore do not involve topographic factors. SWAT (Arnold et al., 1998) is a lumped model in which each subwatershed is associated to a unique radiation gauge. Here, topographic corrections are not considered and the measured solar radiation data, when available, are directly applied on the whole region of influence by means of estimated extraterrestrial radiation. MIKE-SHE (Refsgaard and Storm, 1995), is a comprehensive, deterministic, distributed and physically-based modelling system capable of simulating all major hydrological processes in the land phase of the hydrological cycle (Singh et al., 1999). However, up to now, atmospheric processes have not generally been modelled explicitly and whereas precipitation is a direct input in MIKE SHE, radiation and water vapour transport in the atmosphere are typically bound up in evapotranspiration models (Graham and Butts, 2005) and usually simple methods, such as Thiessen polygons or other areal methods, are applied to extrapolate the point scale values for the referred stations at a watershed scale (Singh et al., 1999; Vázquez et al., 2002; Vázquez and Feyen, 2003).

The aim of this study is to address the importance of incorporating in hydrological models the effects of topography on the spatial distribution of global solar radiation at watershed scale. To this purpose, different topographic algorithms have been coupled in order to estimate series of distributed solar radiation values and calculations have been made to quantify such influence on evapotranspiration estimates in mountainous areas in Mediterranean locations. Thus, an algorithm was derived from Dozier (1980) and Jacovides et al. (1996) to take into account the lack of meteorological stations at high altitudes. To be exact, it should estimate hourly global values as well as the separation between its beam and diffuse components from the common measurements obtained on horizontal surfaces. The resulting algorithm was implemented on a GIS-based routine and applied to data from a mountainous watershed on the south coast of Spain. The distributed results were compared to those obtained from simpler interpolating methods and experimental data. Finally, in order to address the hydrologic importance of using topographically corrected solar radiation fields over uniform values, a simple evaluation in terms of their influence in the computation of reference evapotranspiration fields is carried out.

2 Materials and methods

2.1 Study area and data sources

The study area is the Guadalfeo river watershed, Southern Spain (Fig. 1), where the highest altitudes in Spain can be found (3 482 m) with the coastline only 40 km away, in a 1 300 km² area which results in the interaction between semiarid Mediterranean and alpine climate conditions, with the regular presence of snow (Díaz, 2007; Herrero, 2007; Aguilar, 2008; Millares, 2008). The combination of such altitudinal gradients together with the large number of vegetation, landforms and soil types produces a complex mountainous terrain with variable hydrological behaviour. The main part of the watershed, in terms of hydrology, is comprised of the southern hillside of Sierra Nevada, where global radiation is high throughout the year due to its aspect and lack of cloud cover, even during winter, despite the cold temperatures and the presence of snow. However, the deep valleys with a characteristic south-facing orientation lead to important differences in the instantaneous global radiation between the east- and west-facing mountain slopes, especially after sunrise and before sunset when these valleys are mainly in the shade.

The meteorological data used in this study consisted of daily datasets provided by the three stations (Fig. 1) of the Agroclimatic Information Network of Andalusia (RIA) available in the watershed: 601, 602 and 603, whose UTM coordinates are shown in Table 1. Measurements were made with a Skye Llandrindod Wells SP1110 pyranometer, with a characteristic range of 0.35~1.1 μm.

The topographic input data are represented by a digital elevation model (DEM) with a horizontal resolution of 30 x 30 m and 1 m of vertical precision (Fig. 1). Surface slope and aspect were calculated for each point in the DEM, using the regression plane through the 3 x 3 neighbourhood of a given point after Dozier and Frew (1990).

For the evaluation of the algorithm performance, the daily datasets applied were provided by one station of the Andalusian Alert and Phytosanitary Information Network (RAIF) (referred as 702 in Fig. 1) which measures the variable with a Skye Llandrindod Wells SP1110 pyranometer, with a characteristic range of 0.35~1.1 μm, as well as hourly data recorded at a new climatological station installed in 2004 in Sierra Nevada by the University of Granada Environmental flow dynamics Research Group at an elevation of 2 510 m (referred as 802 in Fig. 1). Measurements of global radiation at station 802 were made with a Kipp and Zonen

SP-Lite pyranometer, with a characteristic range of 0.4~1.1 μm. The sensor was placed on a horizontal surface, partially surrounded by higher ground to the north but completely exposed to the south.

2.2 Calculation of solar radiation components

The global radiation flux (R_g) aimed at a given location at a given moment is the sum of three components: direct or beam radiation (R_b), diffuse radiation (R_d) and reflected radiation from surrounding bodies (R_r).

The amount of radiation reaching the top of the atmosphere is inversely proportional to the square of the distance to the sun, which is a fairly straightforward geometric procedure. The solar constant (I_{CS}) is the rate at which solar energy affects a unit surface, at a normal angle to the sun's rays, in free space, at the earth's mean distance from the sun. In fact, I_{CS} is not a constant value but it can be fixed around 1 367 Wm^{-2} (Frölich and Brusa, 1981) for practical purposes. For the extraterrestrial radiation incident upon a horizontal unit surface normal to the sun's rays (R_{on}), in other words, the radiation which would be incident on the same horizontal surface in the absence of any atmosphere, I_{CS} is corrected with the eccentricity factor (E_o) to account for the changes in distance from the earth to the sun along the elliptical trajectory, according to the expressions in Iqbal (1983).

$$R_{on} = E_o \cdot I_{CS} \quad (1)$$

Finally, for the extraterrestrial radiation incident upon a horizontal surface located at an angle relative to the sun's beams (R_o), the solar coordinates (Fig. 2), the zenital angle (θ_z) or its complementary angle, the sun elevation angle (h_s), and the solar azimuth (ψ) have to be previously defined:

$$R_o = R_{on} \cdot \sin(h_s) = R_{on} \cdot \cos\theta_z \quad (2)$$

Solar coordinates, which are calculated following the equations in Iqbal (1983), are functions of geographical latitude (ϕ_L), and solar declination (δ). Solar declination, or the angle between the line joining the centers of the earth and the sun and the plane of the Equator, varies from -23.5º to +23.5º during the year; however, as the maximum variation in one day is never higher than 0.5º (at the equinoxes), a constant daily value can be used, which is the value at the noon (Iqbal, 1983).

In order to obtain the total amount of global radiation during a day, extraterrestrial radiation must be integrated from sunrise to sunset. Daily extraterrestrial radiation values depend on the terrestrial coordinates but, as a medium-sized watershed, unique values for latitude and longitude were considered and therefore a constant daily value of extraterrestrial solar radiation was obtained for the whole watershed.

2.2.1 Beam and diffuse component estimation on horizontal surfaces

The correlation applied in the present study, shown in Eq. (3) and based on the clearness index (*CI*), was obtained by Jacovides et al. (1996), who investigated the accuracy of some of the previously available correlations when applied locally for high-quality data registered in Cyprus, and found that such correlations are location-independent. However, they developed a specific correlation which is more suitable for applying in Mediterranean areas:

$$R_d/R_g = \begin{cases} 0.992 - 0.0486CI & CI \le 0.1 \\ 0.954 + 0.734CI - 3.806CI^2 + 1.703CI^3 & 0.1 \le CI \le 0.71 \\ 0.165 & CI \ge 0.71 \end{cases} \quad (3)$$

Beam daily solar radiation (R_b) can be obtained as the difference between global and diffuse radiation:

$$R_b = R_g - R_d \quad (4)$$

The application of hourly relations between hourly *CI* and hourly diffuse radiation values was initially considered following previous work in the literature (Orgill and Hollands, 1977; Bugler, 1977; Erbs et al., 1982). However, the aim of this work was to provide a feasible method to include topographic effects on radiation at watershed scale, and the size and heterogeneity of the study site together with the lack of meteorological stations, which unfortunately are usual circumstances in many locations, make it unreasonable to spatially interpolate hourly *CI* values as the spatial distribution of diffuse and direct radiation shows a better correlation at a daily scale. Besides, the application of hourly correlations would require the availability of some other variables such as solar altitude or air mass (González and Calbó, 1999). However, as pointed out by Zaksek et al. (2005), the use of more sophisticated models depends on the scale and purpose of the study, so that under certain circumstances it would be better to use a less complex model. Thus, a simpler approach is proposed so that once the daily values of each component are obtained for each cell, the hourly values (r_b and r_d), are computed by distributing the daily amounts along the day following the temporal pattern of extraterrestrial hourly radiation during the day. The hourly

values of beam and diffuse radiation on horizontal surfaces can then be transposed to give hourly radiation on tilted surfaces, since hourly methods of computing radiation on inclined planes, when available, should give slightly more accurate results than those obtained by the daily methods (Iqbal, 1978).

2.2.2 Conversion from estimates on horizontal surfaces to tilted surfaces

With $\tau(\omega)$ a dimensionless transmission coefficient of the atmosphere for beam radiation on an horizontal surface, the following relationship between hourly beam values (r_b) and extraterrestrial radiation (r_o) for a certain hour angle (ω) both on an horizontal surface, is established (Iqbal, 1983):

$$r_b = \tau_b(\omega) r_0 \tag{5}$$

The same approximation, under the isotropic assumption on a randomly-oriented surface yields:

$$r_{b,\beta\gamma} = \tau_b(\omega) r_{0,\beta\gamma} \tag{6}$$

with $r_{b,\beta\gamma}$ as the hourly beam radiation on a surface of slope β and orientation γ, and the same for the hourly extraterrestrial radiation ($r_{o,\beta\gamma}$) on a randomly-oriented surface. By replacing the transmission coefficient, the following expression for the estimation of $r_{b,\beta\gamma}$ in terms of the zenital angle (θ_z) and a new corrected zenital angle for the sloping surface (θ) is obtained:

$$r_{b,\beta\gamma} = (r_b / r_o) r_{0,\beta\gamma} = r_b(\cos\theta / \cos\theta_z) \tag{7}$$

Therefore, for the calculation of hourly beam solar radiation on tilted surfaces, a correction in the solar coordinates is necessary, so that the cosine of the zenital angle includes the effect of slope and orientation. Such corrected zenital angle or illumination angle (θ), function of the sun-earth-tilted surface geometrical relationship, can be obtained as (Iqbal, 1983; Allen et al., 2006):

$$\begin{aligned}\cos\theta = {} & \sin\delta \cdot (\sin\phi_L \cdot \cos\beta - \cos\phi_L \cdot \sin\beta \cdot \cos\gamma) + \\ & \cos\delta \cdot \cos\omega \cdot (\cos\phi_L \cdot \cos\beta - \sin\phi_L \cdot \sin\beta \cdot \cos\gamma) + \\ & \cos\delta \cdot \sin\beta \cdot \sin\gamma \cdot \sin\omega\end{aligned} \tag{8}$$

2.3 Modelling topographic effects

The topographic effects on solar radiation are mainly variations in the illumination angle and shadowing from local horizons, the apparent intersection of the earth and the sky as seen by an observer in a certain direction. The local horizon information from the gridded data allows us to ascertain whether a given location at a certain sun position is shaded from direct sunlight by surrounding terrain and determines, at any location, the portion of the overlying hemisphere which is obscured by the terrain (Dozier et al., 1981; Dubayah, 1992). Thus, each hourly component, beam, diffuse and reflected radiation is calculated separately to account for the topographic effects (González-Dugo et al., 2003).

According to Essery and Marks (2007), even though since the availability of gridded data and powerful computers many efficient algorithms for calculating distributions of solar radiation over topographic grids have been developed, all of them implement the same basic geometric principles. Thus, the calculation of horizons in this study was made following the modification to the method by Dozier (1980), made more computationally efficient by Dozier et al., (1981) and Dozier and Frew (1990). They developed a simple and fast algorithm for the extraction of horizons from DEMs by comparing slopes between cells in a certain direction, and formulated the problem by determining the coordinates of the points which constitute the horizons in each cell. Then, by rotating the matrix and solving it in a one-dimensional way along each row as many times as directions are considered, they derived the horizons in the whole hemisphere for each cell in the DEM. In this study, eight directions were considered in the calculation: the four cardinal points and their mid-way points.

2.3.1 Beam radiation

This fraction is strongly influenced by the illumination angle. Therefore, the main factors conditioning the fraction of beam radiation are not only the slope and aspect of the location relative to its neighbours, but also the location of the sun relative to the slope at each time step. A certain location is receiving direct sunlight if none of the following situations are taking place:

- Self-shadowing due to its own slope: this takes place if the vector normal to the surface forms an angle greater than 90° with the solar vector (González-Dugo et al., 2003) (e.g. north-facing hill slope and 45° slope, sun in the south at 30° over the horizon). This situation is easy to calculate, as Eq. (8) yields a negative value.

- Shading cast by the nearby terrain: in this case, the sun is hidden by a local horizon. This case is more complex, since, unlike slope and orientation, it can not be calculated with information restricted to the immediate neighbourhood of a given point (Dozier et al., 1981). In order to express it mathematically, the term known as horizon angle in a certain direction ϕ, H_Φ, is introduced as the angle between the normal to the surface and the line joining such point or grid in the DEM with another point in the same direction high enough to block solar radiation. Thus, shading by the surrounding terrain will occur for each time step if the illumination angle is greater than the horizon angle in that direction.

2.3.2 Diffuse radiation

Topography influences the diffuse component by modifying the portion of the overlying hemisphere visible at a certain point. The computation of scattered and reflected radiation fluxes from the atmosphere to the slopes is rather complicated, owing to the fact that the fluxes are considerably non-isotropic. A common assumption made is that the diffuse component of solar radiation (sky light) has an isotropic distribution over the hemispherical sky. However, the non-isotropic character of diffuse radiation fields (maximum intensities near the sun and the horizons, minimum intensities in the direction normal to that of the sun, etc) makes the simplified assumption sufficiently unrealistic to introduce errors into calculations of the energy incident on sloping surfaces (Temps and Coulson, 1977). Nevertheless, following the ideas of Kondratyev and Manolova (1960), who concluded that the isotropic approximation is sufficient for practical purposes (Klutcher, 1979), the isotropic assumption will prevail in this study with the portion of overlying hemisphere visible at each cell as the main factor controlling this component. Thus, the hourly diffuse radiation ($r_{d,\beta\gamma}$) on a surface of slope β and orientation γ, is:

$$r_{d,\beta\gamma} = r_d \cdot SVF \tag{9}$$

where the sky view factor, *SVF*, is the ratio between the diffuse component at one given point and that on an unobstructed horizontal surface, so it corrects the incoming flux incident on a flat surface to flux over a sloping and possibly obstructed surface (Dubayah, 1992). Under the assumption of isotropic sky, a constant value for the *SVF* can be expressed analytically, in terms of the different horizons in each direction considered, as (Dozier and Frew, 1990):

$$SVF = \sum_{\phi=1}^{8} \cos\beta \cdot \sin^2 H_\phi + \left(\sin\beta \cdot \cos\gamma\left(H_\phi - \sin H_\phi \cos H_\phi\right)\right) \tag{10}$$

2.3.3 Reflected radiation

Albedo refers to the global reflectance of the surface to solar radiation. Both albedo and topography can vary over short distances, and their interaction can lead to a wide variability in global solar radiation on a scale of meters (Dubayah, 1992). Reflected radiation can be computed following the ideas of Dozier and Frew (1990) from:

$$r_{r,\beta\gamma} = \rho \cdot \left[\left((1+\cos\beta)/2\right) - SVF\right] \cdot \left(r_{d,\beta} + r_{b,\beta}\right) \qquad (11)$$

where the term in brackets represents the terrain configuration factor for isotropic conditions and infinitely long slope, and ρ is the albedo of the surface. The spatial average of albedo is a factor which is difficult to estimate (Tasumi et al., 2006). In this study, the albedo was estimated by Díaz et al. (2007) from the remote sensing data available from Landsat-5 and Landsat-7 satellites during the study period. After the images have been properly corrected and their reflectivity values extracted, albedo values are obtained at the cell scale through the method proposed by Brest and Goward (1987) and interpolated for the whole time lapse on a daily basis.

2.3.4 Global radiation

Finally, global radiation at an hourly scale is obtained as the sum of each component at an hourly scale once: (1) direct irradiance has been corrected by self-shadowing and shadows cast by nearby terrain; (2) diffuse sky irradiance has included the portion of the overlying hemisphere that may be obstructed by nearby terrain, and (3) direct and diffuse irradiance reflected by nearby terrain towards the location of interest have been calculated from both corrected components (Dubayah, 1994).

2.4 Evaluation of the topographic effects on solar radiation fields on reference evapotranspiration estimates

The choice of a method for the calculation of ET_0 depends on numerous factors. The available energy at the soil surface is the first control of the process, so the estimation of this factor from available data sometimes conditions the method (Shuttleworth, 1993). In this study, the ASCE-Penman Monteith equation (Eq. (12)) was applied for the estimation of evapotranspiration over a reference surface (Allen et al., 1998):

$$ET_0^{ASCE} = \frac{0.408\Delta(R_n - G) + \gamma \frac{C_n}{T + 273.16} u_2 (e_s - e_a)}{\Delta + \gamma(1 + C_d u_2)} \quad (12)$$

where ET_0^{ASCE} is the reference evapotranspiration during a certain time step (mm/Δt); Δ the slope of the vapour pressure-temperature-curve saturation calculated at mean air temperature (kPa/ºC); γ the psychrometric constant (kPa/ºC); R_n and G the net radiation (combination of net shortwave and net longwave radiation) and soil heat fluxes, respectively, both in mm/Δt water equivalent; e_a and e_s the actual and saturation vapour pressure (kPa), respectively; T the daily mean air temperature (ºC) and u_2 the wind speed, both measured at a height of 2 metres above the soil surface (m/s). Finally C_d and C_n are resistance coefficients which vary with the reference crop, temporal time-step and, in the case of hourly time-steps, with daytime and night time. Here, the daily time step was applied and so the values of C_d and C_n were 900 and 0.34 respectively.

The calculation of some of the variables involved in the ASCE-PM equation can be found in detail depending on the available input data in Allen et al. (1998). Saxton (1975) found out that the variable to which the equation is most sensitive is net radiation. Net short-wave radiation (Eq. (13)) on the soil surface, as the difference between incident and reflected radiation, can be expressed in terms of the albedo of the surface, α (0.23 for the reference surface) and the predicted incoming solar global radiation, R_g (MJ/m^2). In the same way, the net long-wave radiation was calculated by Eq. (14) where ε_{atm} and ε_{sup} are the atmospheric and surface emissivity respectively, T (K) the mean air temperature, T_{sup} (K) the temperature of the soil surface and σ Stefan-Boltzmann's constant ($4.903 \cdot 10^{-9}$ MJ/K^{4}m^{2}day). The atmospheric emissivity was calculated through a parametric expression by Herrero et al. (2009) based on near-surface measurements of solar radiation and relative humidity, valid for the local conditions of the study area. As ε_{sup} ranges from 0.985 in cotton crops to 0.94 in bare soil (Stefano and Ferro, 1997), a constant value of 1 was assumed. Besides, as soil temperature is not commonly available at broad scales it is assumed to be equal to the temperature of the air, an so the expression for net long-wave radiation remains as previously done by other authors (Doorenbos and Pruitt, 1977; Allen, 1986; Allen, 1998) as a modification to Stefan-Boltzmann's law due to the absortion and downward radiation from the sky. Thus, the product of the Stefan-Boltzmann's constant times the fourth power to the mean air temperature is modified with a cloudiness factor and an air humidity factor (Allen et al.,

1998; Donatelli et al., 2006), both factors included in this study in the term ε_{atm} and so, together with the mean air temperature constitute the only inputs to the equation.

$$R_{ns} = (1-a)R_g \quad (13)$$

$$R_{nl} = \varepsilon_{atm} \cdot \sigma \cdot T^4 - \varepsilon_{\sup} \cdot \sigma \cdot T_{\sup}^4 \approx (\varepsilon_{atm} - 1) \cdot \sigma \cdot T^4 \quad (14)$$

Finally, as the algorithm is able to derive global radiation values at the cell scale and once the rest of inputs to the ASCE-PM equation are also available at the cell scale (Herrero et al., 2007) the influence of topographic effects is evaluated in a distributed manner in ET_0^{ASCE}, estimated after using the topographically corrected values in comparison with distributed estimates by IDW of the solar radiation data registered at the meteorological stations.

3 Results and discussion

In order to run the proposed set of algorithms at the watershed scale, hourly global radiation was calculated from each 30 x 30 m^2 cell of the DEM in the study area for the period comprised between 4 November 2004 and 29 April 2007.

The results are organised into three sections. Firstly, comparisons of the results obtained through the topographic radiation algorithm previously exposed with those derived from a classical interpolation technique are showed. Secondly, the suitability of the results at different temporal scales is presented through its comparison with field measurements, proving the accuracy of the estimated values for hydrological distributed modelling. Finally, in order to address the hydrologic importance of using topographically corrected solar radiation fields over uniform values obtained through classical interpolation techniques, the influence of both estimations as inputs to reference evapotranspiration computations is evaluated.

3.1 Topographic corrections vs classic interpolation techniques on solar radiation estimates

At the first stage, topographic information was derived from the DEM (Fig. 1) in the study area. Slope and orientation maps were obtained and the horizons for each cell were calculated as stated before. Once these parameters are available for a certain area they can be used in subsequent executions as they are considered to be independent of the time of the year.

In order to compare the results obtained through the topographic algorithm with those of classic interpolation techniques, a reference day was selected. This date, 20/11/2004 was chosen as it was cloudless and it had not rained for several days. This condition is very important for the albedo estimation from remote sensing images, as the presence of moisture in the environment influences the quality of the estimates and therefore consecutively dry days are most suitable for an accurate performance. Moreover, remote sensing images were available for this date and therefore the errors due to the temporal interpolation of albedo values were minimized.

Combining the daily extraterrestrial value over a flat surface on the selected date (17.85 MJ/m^2day) with the global radiation registered in the measuring network, which can be seen in Table 1, the clearness index was obtained for each station and spatially interpolated following the inverse distance weighed (IDW) method, in order to distribute it throughout the watershed. This may appear to be quite an unrealistic simplification, but it is justified by the lack of more spatially distributed registering sites which would allow to look into the factors that affect the *CI* such as the variation in the atmospheric air mass through the height of each cell, distance to the coast, etc. Therefore future research is proposed into the spatial distribution of this index while a simple spatial interpolation technique is applied as a first approximation in the present study.

Once the mean daily clearness index was spatially derived, global radiation values were divided into its beam and diffuse components over a flat surface at a cell scale, and distributed according to the hourly extraterrestrial radiation values for the subsequent topographic corrections. Finally, the hourly sequence of global radiation, as the sum of each component at an hourly scale once each component has been properly corrected, is shown in Fig. 3a, where the spatial gradient in hourly global radiation is evident. On the whole, it can be seen that the locations receiving more radiation are those in the highest part of the watershed, with a south-facing orientation that remains unobstructed during most of the hours of daylight.

In order to assess the potential of the topographic corrections, a simple interpolation technique was applied for the same date. For this, the inverse distance weighed was applied to the hourly values of global radiation measured in the stations (Fig. 3b). From contrasting results between Figs. 3a and 3b, not only was a huge difference visible in the distributed values of the variable cell by cell, but also the wider range of global values in the watershed, when topographic factors are taken into account. In this latter case, extreme values, far exceeding

the measured values, represent extreme conditions, such as high areas remaining unobstructed most of the daytime and sometimes receiving almost double the values obtained through interpolation of the data recorded at the stations or, at the other end of the scale, valleys that receive minimal or even zero null quantities of solar radiation, due to the configuration of the surrounding terrain. As a consequence, processes such as evaporation or snowmelt, which rely heavily on solar radiation, can be miscalculated under a wide range of conditions, such as overestimations in areas obstructed by nearby terrain or underestimations in the upper and exposed regions of the watershed, among others.

Hourly values can be aggregated in each cell at the required temporal scale. In this way, Fig. 4 represents the spatial distribution of daily global radiation on 20/11/2004 estimated through the topographic algorithm (Fig. 4a) and from IDW (Fig. 4b), respectively. Again, the same ideas can be drawn as at an hourly time step, since maximum and minimum values found in the watershed considering topographic effects are quite different to those obtained through IDW and the daily values registered at the meteorological stations (Table 1). In this way, we found differences of as much as an extra 60% in the estimated daily values compared with those obtained through spatial interpolation without consideration of topography, predominantly on the south-facing hillsides in the northern part of the watershed, and estimates of up to 90 % of lower in certain cells obstructed most of the daytime.

Finally the same comparison for the hydrological year 2004, from 1 September 2004 to 31 August 2005 (Figs. 4c and 4d) resulted in a mean excess of 324 MJ/m^2/year with a standard deviation of 850 MJ/m^2/year when applying IDW over the topographic computation and extreme differences of the same order of magnitude as at the daily time step.

3.2 Validation of topographic corrections

The radiation values generated were compared against the radiation measurements and the agreement between generated and measured data was evaluated through 1:1 lines. The period considered in the evaluation was determined by the availability of data in the climatological station 802, which included almost two and a half hydrological years, from 4 November 2004 to 29 April 2007.

As regards daily values, a close agreement between generated (R_{gp}) and measured (R_{go}) values can be observed in Fig. 5 as points tend to line up around the 1:1 line. However, a slight underestimation in the generated values can also be appreciated, with the topographic

approximation underestimating the values measured at stations 702 and 802 by 6 and 7% respectively. Such underestimations take place especially in summer periods, as depicted in Fig. 6, when the availability in this study of remote sensing images for an accurate estimation of albedo was more limited, and also on very clear days, when an increase in global radiation with altitude is expected, due to the reduction in density of the atmosphere, and when the consideration of anisotropy in the atmosphere would modify the estimation of the diffuse component. In this way, the consideration of factors creating spatial gradients in the distribution of the *CI*, such as altitude, distance to the coast or proximity to urban areas, could improve the results in our study, especially in very cloudless days and considering that the climatological stations used to estimate the *CI* are located at relative low elevation compared to the mean height of the watershed.

To conclude, the accuracy of predicted hourly values was assessed in station 802, where measurements at this time scale were available. Despite the scattering effect observed in Fig. 7, which shows the agreement between predicted (r_{gp}) and measured (r_{go}) hourly values for the evaluation period, we can say that the algorithm reasonably predicts the observed data with a R^2 of 0.83, especially considering the time scale and some of the assumptions of the algorithm which at this time step might appear rather simplistic. In this way, the installation of a denser monitoring network provided with solar devices recording hourly direct and diffuse radiation data may improve the results. Firstly, it would provide the spatial scheme required for the spatial interpolation of hourly values. Secondly, it would allow including more factors for the spatial distribution of the *CI* as previously suggested. Finally, the derivation of hourly correlations between the hourly diffuse radiation and the *CI* would be reasonable in the study area. To sum up, the possibility to work at finer scales would be the ideal as the geometrical relationships involved in the calculation of extraterrestrial radiation are continuous in time. However, independently of this continuous nature of extraterrestrial radiation, the time scale of the computation of the incoming solar radiation is determined by the temporal frequency of the monitoring network. Nevertheless, the calculations with aggregated hourly values at higher temporal scales such as the daily time step showed the same degree of detail that at hourly time scale (R^2 around 0.8).

Finally, since cloudless skies are required for an accurate characterization of the albedo from remote sensing images, the results at an hourly time step were analysed considering this effect. Thus, two different atmospheric situations in terms of the occurrence of rainfall are

defined as an indicator of the cloudiness in the atmosphere: events (when it rains somewhere in the watershed) and non-events (periods between events). Fig. 8 represents hourly values for event days on the left-hand side (a, b, c) and non-events on the right (d, e, f).

Table 2 shows different linear fits for each day represented in Fig. 8 and its calculated R^2 values. As was expected, the predicted values were much better for cloudless skies or non-events, when acceptable R^2 values were obtained even when forcing the adjustment to reach the origin. However, as with daily values, the algorithm slightly underestimated the observed hourly values, which following the ideas of Ineichen and Pérez (2002) could be improved with the consideration of the variation of atmospheric density with altitude, as the data used for the calibration are registered at a climatological station located at a height of 2 510 meters. In any case, the worst fits obtained in situations when events occur are expected to be more closely related to the separation of the different components in the global radiation value than to the topographic interpolation process.

Nevertheless, these results are considered to be acceptable in the framework of the present study as the estimation of global radiation in semiarid environments is especially important for cloudless days, when evaporative processes and snowmelt must be considered in water and energy balance modelling. This is especially true considering that cloudless days constitute a higher rate than cloudy days associated to situations when events occur in a Mediterranean area like the present study site: in this case around 75% of clear sky days for the evaluation period.

3.3 Influence of the inclusion of topographic corrections on hydrological variables: ET_0

Finally, a distributed computation of ET_0 was applied for the same reference day of Sect. 3.1 (Fig. 9a) and the hydrological year 2004 (Fig. 9c) (1 September 2004 to 31 August 2005) once all the variables involved in the ASCE-PM equation had been spatially derived including topographic effects. Besides, the ASCE-PM equation was computed with solar radiation surfaces obtained through IDW of the data registered at the stations as inputs to the equation (Figs. 9b and 9d) in order to prove the importance of solar radiation fields which include topographic corrections. Again, in Figs. 9a and 9c not only the apparent spatial variability of ET_0 estimates cell by cell which follows the topographic gradient can be seen, but also a wider range of values in the watershed than with IDW-interpolated solar radiation fields as

inputs (Figs. 9b and 9d). Besides, in this latter case, ET_0 estimates in the watershed appear to be more influenced by the spatial distribution of other variables than by solar radiation (e.g. temperature in Fig. 9b). Considering the mean statistics of the difference between both computations on an annual basis, a mean excess of 62 mm/year and a standard deviation of 142 mm/year in ET_0 estimations when using IDW-interpolated solar radiation fields were obtained. These differences in an area where the mean annual rainfall varies from 450 mm/year on the coast to 800 mm/year on the highest peaks may constitute a considerable source of error in the water balance when applying distributed hydrological models for the management and planning of water resources.

4 Conclusions

Difficulties are sometimes encountered in utilizing available solar radiation data, since they consist primarily of total (direct plus diffuse) radiation only, and the knowledge of the values for each component is often required, especially for the consideration of topographic effects as they affect each component differently.

Thus, detailed time-series radiation surfaces have been developed, using limited data and relatively simple methods, to drive distributed energy and water balance models in mountainous Mediterranean environments. The interpolation is managed through linear interpolation of *CI* as a clue to mean daily radiation, plus topographic properties geometrically related to the sun's position at hourly intervals. Such calculations are easy to reproduce from standard climatological station datasets. The significant incidence of topography on the values of global solar radiation throughout the watershed has been demonstrated by the results of the topographic solar radiation algorithm proposed. In this way, differences of as much as an extra 60% in the estimated daily values compared with those obtained through spatial interpolation without consideration of topography, and estimates of up to 90 % of lower in certain cells obstructed most of the daytime were found. This affects the modelling of the slow but extreme drying out of the watershed during periods between events and the modelling of the snowmelt in the highest areas, among other processes.

The simulated results fit well with the measured values of global radiation at the 2 510 meter high monitoring point established for this work, with a correlation of 0.7 for daily values, and an underestimation of 10% in days with extreme conditions, that decrease the validity of the

assumptions taken in the algorithm, as the previous paragraphs have justified. However, the simulated results constitute a further approach to the accurate characterization of the spatial distribution of hourly global radiation values in mountainous areas with scarce data registering sites. On-going work will develop a further approach, and test the inclusion of additional corrective terms through the establishment of two additional meteorological stations equipped with pyranometers at points with increasing height above sea-level and distance from the sea.

The importance of considering the topographic gradients in the spatial distribution of solar radiation for the study of hydrological processes in which this variable plays a cruciant role became evident against ET_0 estimates with solar radiation fields obtained through classical interpolation techniques of data registered at meteorological stations. In this way, a mean excess of 62 mm/year was found with IDW-interpolated solar radiation fields as inputs to the ASCE-PM equation.

Two final comments are included on the applicability of the algorithm proposed in this work. For the purposes of computer simulation programs, which handle vast amounts of data, this algorithm was implemented in Matlab during the trials and finally in C++ to get a sufficiently fast computation, considering all the processes involved at a cell scale. Besides, some of the assumptions that could appear quite unrealistic due mainly to the scarcity of data, have managed to achieve a compromise between a sufficiently representative distributed approximation and a high-speed processing algorithm that can be run on a desktop PC, from the comparison with measured data and simpler interpolation techniques. Finally, through the use of daily samples, the availability of data is enhanced as not many hourly registers are needed; this allows the use of the algorithm in mountainous areas which lack a high frequency monitoring network, which is so common in many other areas.

Acknowledgements

This work was funded by the Andalusian Water Institute in the project *Pilot study for the integral management of the Guadalfeo river watershed* and by the Regional Innovation, Science and Enterprise Ministry grant for PhD training in Andalusian Universities and Research Centers.

References

Aguilar, C.: Scale effects in hydrological processes. Application to the Guadalfeo river watershed (Granada). PhD Thesis. University of Córdoba, http://www.cuencaguadalfeo.com/archivos/Guadalfeo/Tesis/TesisCris_en.pdf, last access date: 5 April 2010, 2008.

Allen, R.G.: A Penman for all seasons, J. Irrig. Drain. Eng. ASCE., 112, 348-368, 1986.

Allen, R.G., Pereira, L.S., Raes, D., and Smith, M.: Crop evapotranspiration, guidelines for computing crop water requirements, Irrig. and Drain. Pap., 56. U.N. Food and Agric. Organ., Rome, 1998.

Allen, R.G., Trezza, R., and Tasumi, M.: Analytical integrated functions for daily solar radiation on slopes, Agric. For. Meteorol., 139, 55-73, 2006.

Antonic, O.: Modelling daily topographic solar radiation without site-specific hourly radiation data, Ecol. Modelling, 113, 31-40, 1998.

Arnold, J.G., Srinivasan, R., Muttiah, R.S., and Williams, J.R.: Large area hydrologic modelling and assessment-Part I: model development, J. Amer. Water Res. Assoc., 34, 73-89, 1998.

Bingner, R.L. and Theurer, F.D.: AnnAGNPS Technical Processes. USDA-ARS. National Sedimentation Laboratory, 2003.

Brest, C.L. and Goward, S.N.: Deriving surface albedo measurements from narrow band satellite data, Intern. J. Remote Sens., 8, 351-367, 1987.

Bugler, J.W.: The determination of hourly insolation on an inclined plane using a diffuse irradiance model based on hourly measured global radiation insolation, Sol. Energy, 19, 477-491, 1977.

Chen, R., Kang, E., Ji, X., Yang, J., and Wang, J.: An hourly solar radiation model under actual weather and terrain conditions: A case study in Heihe river watershed, Energy, 32, 1148-1157, 2007.

Collares-Pereira, M. and Rabl, A.: The average distribution of solar radiation--Correlations between diffuse and hemispherical and between daily and hourly insolation values, Sol. Energy, 22, 155-164, 1979.

Cronshey, R.G. and Theurer, F.D.: AnnAGNPS—Non-Point Pollutant Loading Model. In: Proceedings First Federal Interagency Hydrologic Modeling Conference, 19-23 April 1998, Las Vegas, NV, pp. 1-9 to 1-16, 1998.

Díaz, A.: Temporal series of vegetation for a distributed hydrological model. Master Thesis (in spanish), University of Córdoba, last access date: 5 April 2010, http://www.cuencaguadalfeo.com/archivos/Guadalfeo/Libros/TFM_Adolfo%20D%C3%ADaz.pdf, 2007.

Diodato, N. and Bellocchi, G.: Modelling solar radiation over complex terrains using monthly climatological data, Agric. For. Meteorol., 144, 111-126, 2007.

Donatelli, M., Bellocchi, G., and Carlini, L.: sharing knowledge via software components: Models on reference evapotranspiration, Europ. J. Agronomy, 24, 186-192, 2006.

Doorenbos, J. and Pruitt, W.O.: Guidelines for predicting crop water requirements, Irrig. and Drain. Pap., 24. U.N. Food and Agric. Organ., Rome, 1977.

Dozier, J.: A clear-sky spectral solar radiation model for snow-covered mountainous terrain, Wat. Resour. Res., 16, 709-718, 1980.

Dozier, J., Bruno, J., and Downey, P.: A faster solution to the horizon problem, Comp. Geosci., 7, 145-151, 1981.

Dozier, J. and Frew, J.: Rapid calculation of terrain parameters for radiation modeling from digital elevation data, IEEE Trans. Geosci. Remote Sens., 28, 963-969, 1990.

Dubayah, R.C.: Estimating net solar radiation using Landsat Thematic Mapper and digital elevation data, Wat. Resour. Res., 28, 2469-2484, 1992.

Dubayah, R.C.: Modeling a solar radiation topoclimatology for the Rio Grande river watershed, J. Veg. Sci., 5, 627-640, 1994.

Dubayah, R. and van Katwijk, V.: The topographic distribution of annual incoming solar radiation in the Rio Grande river basin, Geoph. Res. Let., 19, 2231-2234, 1992.

Erbs, D.G., Klein, S.A., and Duffie, J.A.: Estimation of the diffuse radiation fraction for hourly, daily and monthly average global radiation, Sol. Energy, 28, 293-302, 1982.

Essery, R. and Marks, D.: Scaling and parametrization of clear-sky solar radiation over complex topography, J. Geophys. Res., 112, D10122, doi:10.1029/2006JD007650, 2007.

Flint, A.L. and Childs, S.T.: Calculation of solar radiation in mountainous terrain, Agric. For. Meteorol., 40, 233-249, 1987.

Fröhlich, C. and Brusa, R.W.: Solar radiation and its variation in time, Solar Phys., 74, 209-215, 1981.

Garen, D. and Marks, D.: Spatially distributed energy balance snowmelt modelling in a mountainous river watershed: estimation of meteorological inputs and verification of model results, J. Hydrol., 315, 126-153, 2005.

González, J.A. and Calbó, J.: Influence of the global radiation variability on the hourly diffuse fraction correlations, Sol. Energy, 65, 119-131, 1999.

González-Dugo, M.P., Chica-Llamas, M.C., and Polo-Gómez, M.J.: Modelo topográfico de radiación solar para Andalucía. In: XXI Congreso Nacional de Riegos, Mérida, pp 53-55, 2003.

Graham, D.N. and Butts, M.B.: Flexible, integrated watershed modelling with MIKE SHE. In: Singh, V.P. and Frevert, D.K.: Watershed Models. CRC Press, Boca Raton, 245-272, 2005.

Herrero, J.: Modelo físico de acumulación y fusión de la nieve. Aplicación a Sierra Nevada (España). PhD Thesis (in spanish), University of Granada, http://www.ugr.es/~herrero, last access date: 5 April 2010, 2007.

Herrero, J., Aguilar, C., Polo, M.J., and Losada, M.: Mapping of meteorological variables for runoff generation forecast in distributed hydrological modeling. In: Proceedings, Hydraulic Measurements and Experimental Methods 2007 (ASCE/IAHR), Lake Placid, NY, pp. 606-611, 2007.

Herrero, J., Polo, M.J., Moñino, A., and Losada, M.: An energy balance snowmelt model in a Mediterranean site, J. Hydrol., 271, 98-107, 2009.

Ineichen., P. and Pérez, R.: A new airmass independent formulation for the Linke Turbidity coefficient, Sol. Energy, 73, 151-157, 2002.

Iqbal, M.: Hourly vs daily method of computing insolation on inclined surfaces, Sol. Energy, 21, 485-489, 1978.

Iqbal, M.: Prediction of hourly diffuse radiation from measured hourly global radiation on a horizontal surface, Sol. Energy, 24, 491-503, 1980.

Iqbal, M.: An introduction to solar radiation. Academic Press Canada, Ontario, 1983.

Jacovides, C.P., Hadjioannou, L., Pashiardis, S., and Stefanou, L.: On the diffuse fraction of daily and monthly global radiation for the island of Cyprus, Sol. Energy, 56, 565-572, 1996.

Kambezidis, H.D., Psiloglou, B.E., and Gueymard, C.: Measurements and models for total solar irradiance on inclined surface in Athens, Greece, Sol. Energy, 53, 177-185, 1994.

Klutcher, T.M.: Evaluation of models to predict insolation on tilted surfaces, Sol. Energy, 23, 111-114, 1979.

Kondratyev, K.J. and Manolova, M.P.: The radiation balance on slopes, Sol. Energy, 4, 14-19, 1960.

Liu, B.Y.H. and Jordan, R.C.: The interrelationship and characteristic distribution of direct, diffuse and total solar radiation, Sol. Energy, 4, 1-19, 1960.

Millares, A.: Integración del caudal base en un modelo distribuido de cuenca. Estudio de las aportaciones subterráneas en ríos de montaña. PhD Thesis (in spanish), University of Granada, http://www.ugr.es/local/mivalag, last access date: 5 April 2010, 2008.

Moore, I.D., Grayson, R.B., and Ladson, A.R.: Digital terrain modelling, a review of hydrological, geomorphological and biological applications, Hydrol. Processes, 5, 3-30, 1991.

Orgill, J.F. and Hollands, K.G.T.: Correlation equation for hourly diffuse radiation on a horizontal surface, Sol. Energy, 19, 357-359, 1977.

Ranzi, R. and Rosso, R.: Distributed estimation of incoming direct solar radiation over a drainage basin, J. Hydrol.,166, 461-478, 1995.

Refsgaard, J.C. and Storm, B.: MIKE SHE. In: Singh, V.P.: Computer Models of Watershed Hydrology. Water Resources Publications, USA, 809-846, 1995.

Ruth, D.W. and Chant, R.E.: The relationship of diffuse radiation to total radiation in Canada, Sol. Energy, 18, 153-154, 1976.

Saxton, K.E.: Sensitivity analyses of the combination evapotranspiration equation, Agric. Meteorol., 15, 343-353, 1975.

Shuttleworth, W.J.: Evaporation. In: Maidment, D.R.: Handbook of hydrology. McGraw-Hill, New York, 4.1-4.53, 1993.

Singh, R., Subramanian, K., and Refsgaard, J.C.: Hydrological modelling of a small watershed using MIKE SHE for irrigation planning, Agric. Water Manage., 41, 149-166, 1999.

Spencer, J.W.: A comparison of methods for estimating hourly diffuse solar radiation from global solar radiation, Sol. Energy, 29, 19-32, 1982.

Stefano, C.D. and Ferro, V.: Estimation of evapotranspiration by Hargreaves formula and remotely sensed data in semi-arid mediterranean areas, J. Agric. Engin. Res., 68, 189-199, 1997.

Susong, D., Marks, D., and Garen, D.: Methods for developing time-series climate surfaces to drive topographically distributed energy- and water- balance models, Hydrol. Processes, 13, 2003-2021, 1999.

Tasumi, M., Allen, R.G., and Trezza, R.: DEM based solar radiation estimation model for hydrological studies, Hydrolog. Sci. Tech., 22, 1-4, 2006.

Temps, R.C. and Coulson, K.L.: Solar radiation incident upon slopes of different orientations, Sol. Energy, 19, 179-184, 1977.

Tian, Y.Q., Davies-Colley, R.J., Gong, P., and Thorrold, B.W.: Estimating solar radiation on slopes of arbitrary aspect, Agric. For. Meteorol., 109, 67-74, 2001.

Vazquez, R.F., Feyen, L., Feyen, J., and Refsgaard, J.C.: Effect of grid size on effective parameters and model performance of the MIKE-SHE code, Hydrol. Processes, 16, 355-372, 2002.

Vázquez, R.F. and Feyen, J.: Effect of potential evapotranspiration estimates on effective parameters and performance of the MIKE SHE code applied to a medium-size catchment, J. Hydrol., 270, 309-327, 2003.

Zaksek, K., Podobnikar, T., and Ostia, K.: Solar radiation modelling, Comp. Geosci., 31, 233-240, 2005.

Table 1. UTM coordinates of the climatological stations, measured daily global radiation and clearness index on the 20/11/2004

Station	X	Y	Z	Rg (MJ/m^2day)	CI
601	483724	4086564	950	12.4	0.69
602	446712	4097327	781	14.4	0.80
603	439612	4066365	49	10.4	0.58
702	451435	4089276	700	13.46	0.75
802	471338	4098246	2510	13.81	0.77

1 Table 2. Linear fits of observed (r_{go}), and predicted (r_{gp}) global hourly radiation (MJ/m^2) at
2 station 802 for certain dates.

3

Equation type	$r_{gp}=a \cdot r_{go}$		$r_{gp}=a \cdot r_{go}+b$		
	a	R^2	a	b	R^2
Events					
a) 4/11/2004	1.26	0.69	1.69	0.34	0.75
b) 4/12/2004	0.40	0.17	0.23	0.26	0.62
c) 5/02/2005	0.88	0.19	0.31	0.71	0.21
Non events					
d) 15/11/2004	0.92	0.92	0.81	0.20	0.95
e) 15/12/2004	0.98	0.81	0.81	0.23	0.87
f) 20/02/2005	0.99	0.72	0.77	0.5	0.80

4

5

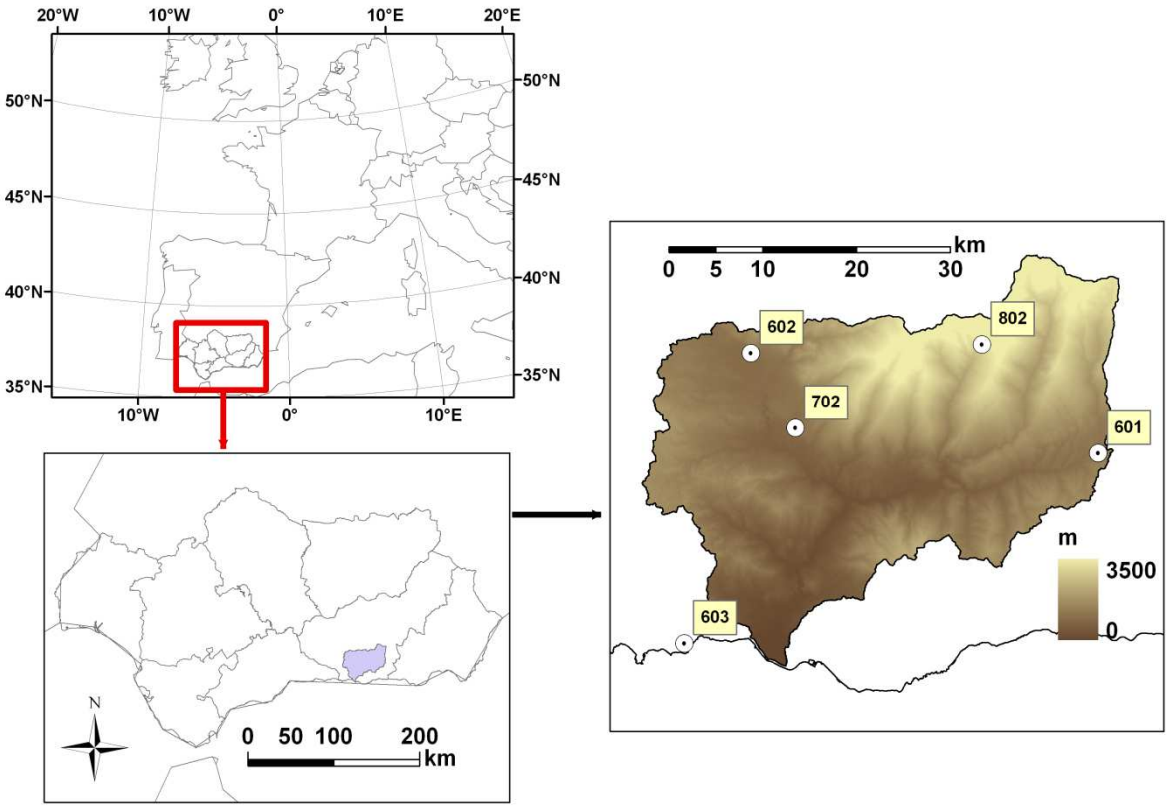

Figure 1. Guadalfeo River Watershed, climatological stations and DEM

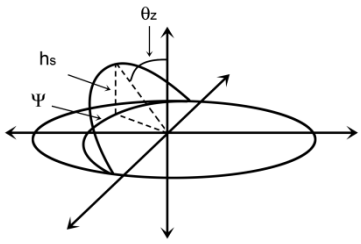

Figure 2. Solar coordinates

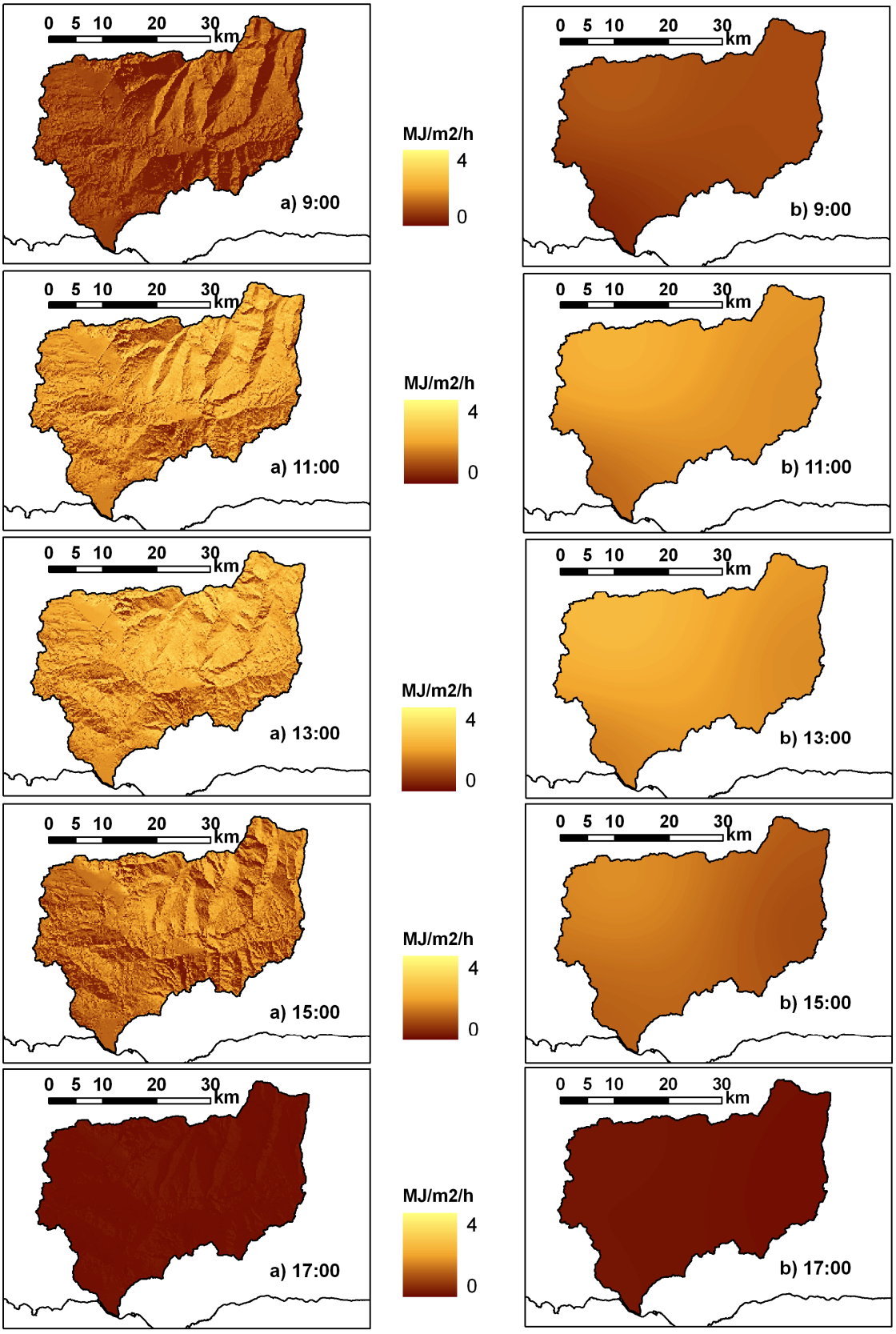

Figure 3. Hourly global radiation (a) topographically corrected vs. (b) IDW interpolated (20/11/2004)

1

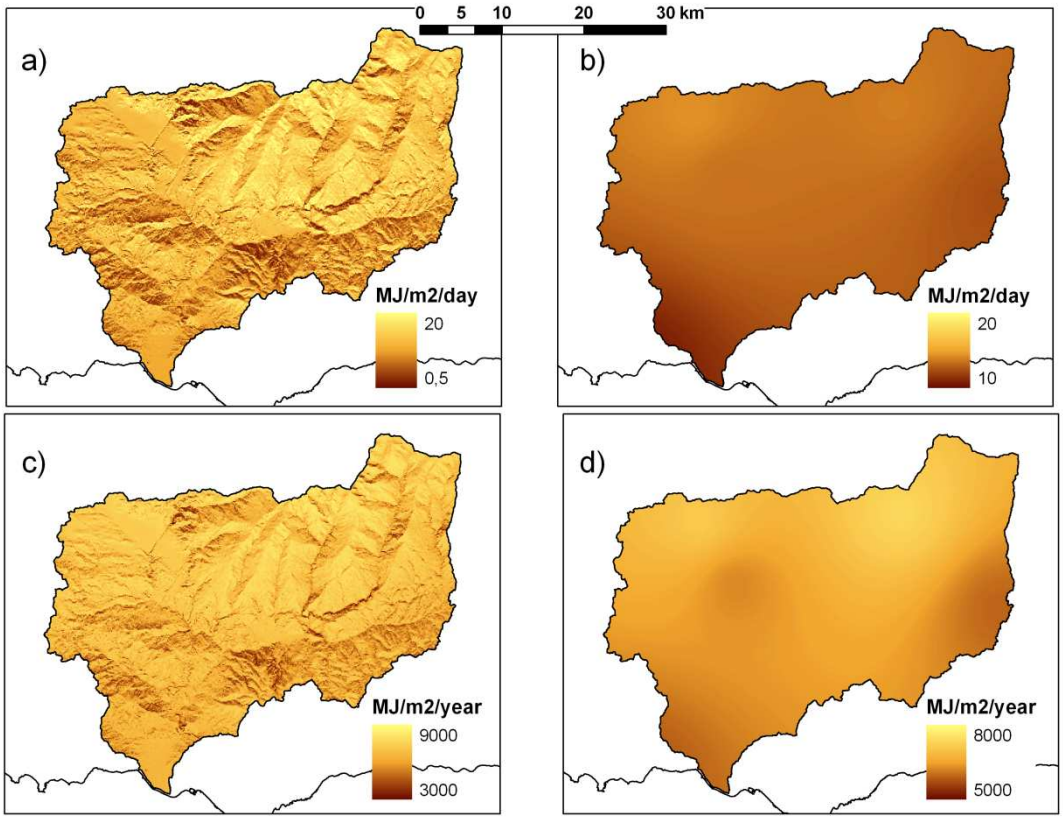

2

3 Figure 4. Daily global radiation (20/11/2004) a) topographically corrected vs. b) IDW
4 interpolated, and annual global radiation (1/09/2004-31/08/2005) (c) topographically
5 corrected vs.(d) IDW interpolated

6

7

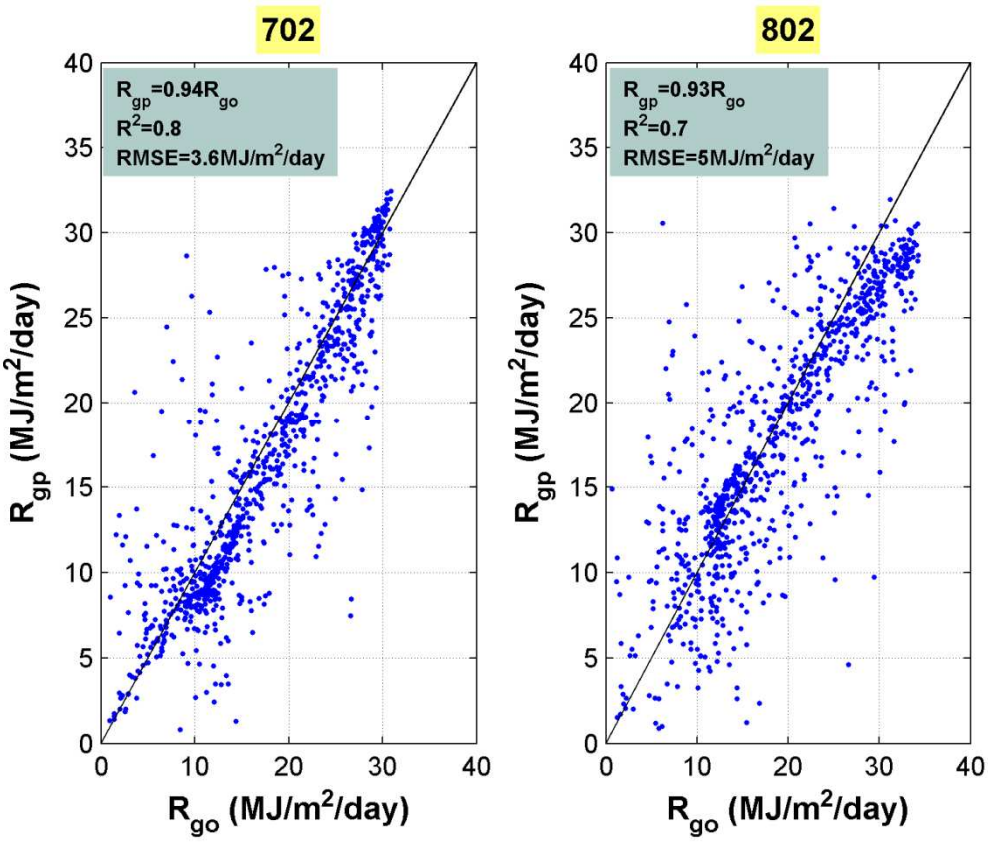

Figure 5. Observed (R_{go}), and predicted (R_{gp}) global daily radiation (MJ/m^2/day) at station 702 and 802 for the evaluation period (4/11/2004-29/04/2007)

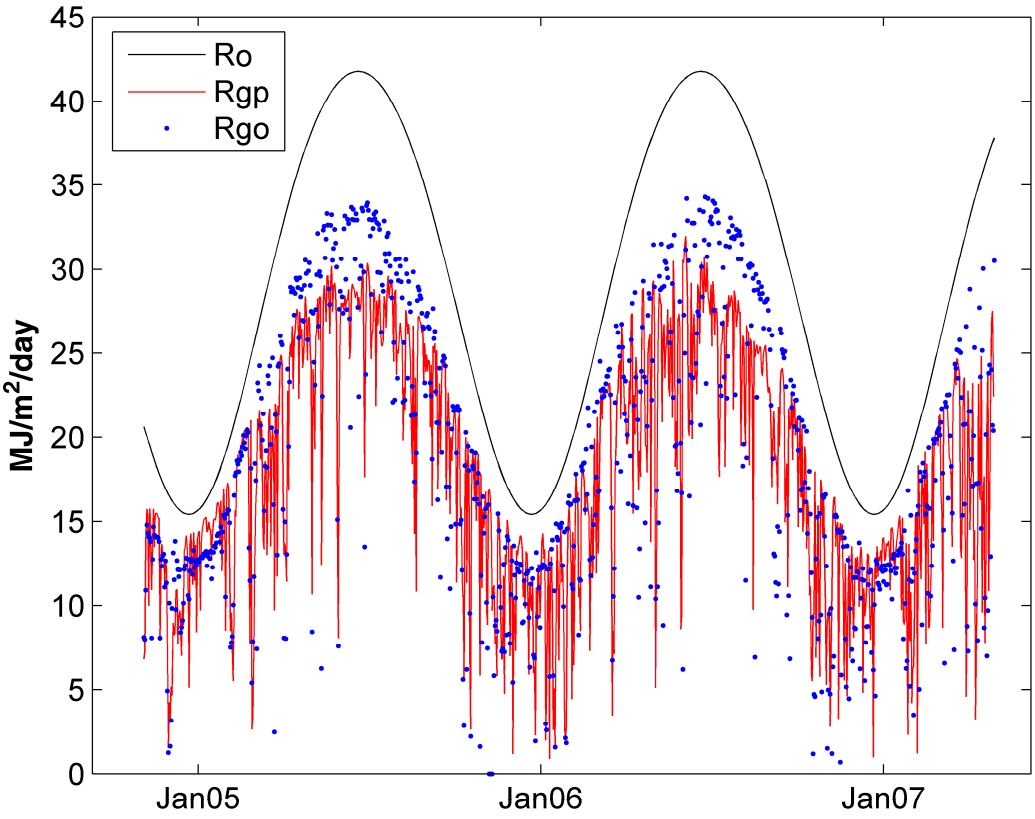

Figure 6. Extraterrestrial solar radiation (R_o), observed (R_{go}), and predicted (R_{gp}) global radiation (MJ/m^2/day) at station 802 for the evaluation period (4/11/2004-29/04/2007)

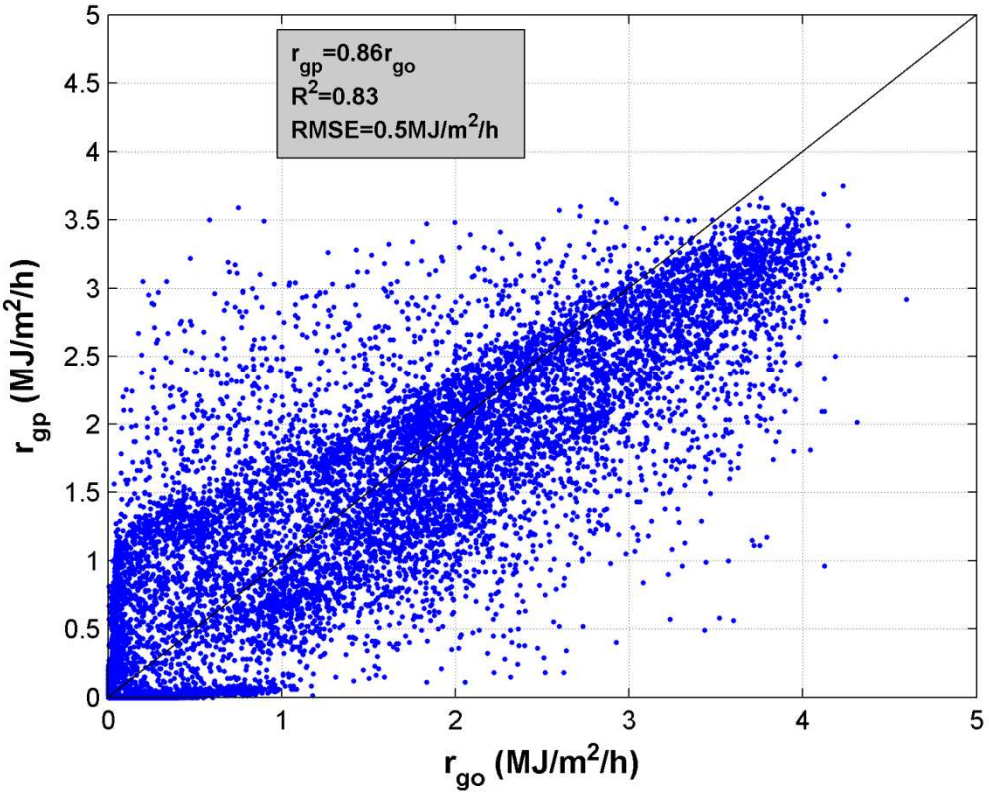

Figure 7. Observed (r_{go}), and predicted (r_{gp}) global hourly radiation (MJ/m^2/h) at station 802 for the evaluation period (4/11/2004-29/04/2007)

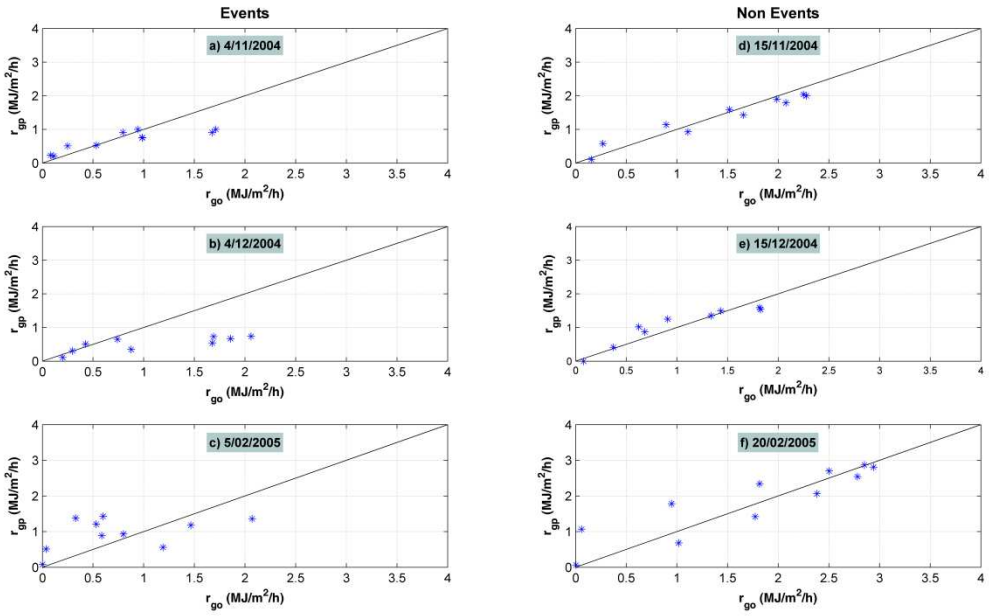

Figure 8. Scatter plots of observed (r_{go}), and predicted (r_{gp}) global hourly radiation ($MJ/m^2/h$) at station 802 for certain dates

1

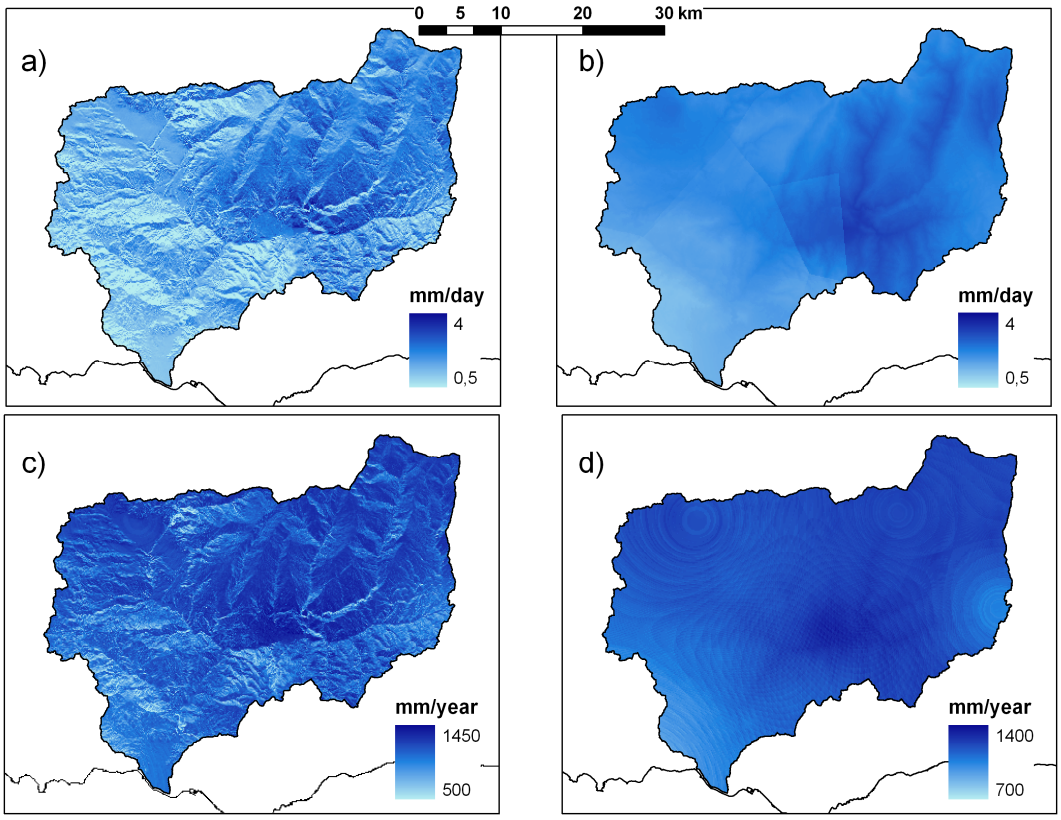

2

3 Figure 9. Daily ET_0 with global radiation (20/11/2004) a) topographically corrected vs. b)
4 IDW interpolated, and annual ET_0 with global radiation (1/09/2004-31/08/2005) (c)
5 topographically corrected vs. d) IDW interpolated

6